

# Observation of near-inertial internal waves in the abyssal Japan Sea

TOMO HARU SENJYU

**Abstract:** Observation with a moored Acoustic Doppler Current Profiler (ADCP) set to a very short measurement interval revealed vertical propagation of near-inertial internal waves (NIW) in the abyssal Yamato Basin in the Japan Sea. Flow and temperature measurements showed a sinusoidal variation having near-inertial period associated with NIW. From the polarization of flow vectors, vertical and horizontal wave numbers of the NIW were estimated to be  $1.741 \times 10^{-3} \text{ m}^{-1}$  and  $2.563 \times 10^{-4} \text{ m}^{-1}$ , respectively. Phase propagation of the NIW was downward at speed of  $5.34 \times 10^{-2} \text{ ms}^{-1}$ , indicating an upward group velocity. Back-tracing of the energy ray path of NIW passing through the observation point shows that the observed NIW were the bottom-reflected waves. The bottom reflected waves were the downward-propagating NIW generated in the upper layer. An event of clockwise rotation of wind vectors was suggested as a cause of the observed NIW.

**Keywords :** *Yamato Basin, ADCP, short measurement intervals, vertical propagation*

## 1. Introduction

Internal gravity waves with frequency close to the local inertial frequency (near-inertial internal waves, NIW) are ubiquitous in the world oceans (WEBSTER, 1968; FU, 1981). NIW have been considered to be an important agent for mixing in the ocean interior (HIBIYA *et al.*, 1996) which controls the intensity of the global-scale thermohaline circulation (TOOLE and McDUGALL, 2001); however, NIW structure and propagation processes in the deep sea have not been clarified.

It is known that the Japan Sea, a semi-enclosed marginal sea in the northwestern North Pacific

(Fig. 1), has its own thermohaline circulation system (GAMO and HORIBE, 1983; SENJYU *et al.*, 2002). NIW have been frequently reported in the Japan Sea not only in the upper layer (KANARI *et al.*, 1987; LIE, 1988; KIM *et al.*, 2001; KIM *et al.*, 2005; PARK and WATTS, 2005; OKEI *et al.*, 2009; IGETA *et al.*, 2009, 2011; BYUN *et al.*, 2010), but also in the deep layer (TAKEMATSU *et al.*, 1999; SENJYU *et al.*, 2005; MORI *et al.*, 2005). Considering that the frequency of internal gravity waves ( $\omega$ ) must be in the band between local inertial frequency ( $f$ ) and buoyancy frequency ( $N$ ) (GILL, 1982), we have some advantages to NIW observation in the Japan Sea. First, the frequency of NIW generated in there is limited to  $0.837\text{--}1.149 \times 10^{-4} \text{ s}^{-1}$ , because of the Japan Sea's latitudinal extent ( $35^{\circ}\text{--}52^{\circ} \text{ N}$ ). Second, deep water in the sea, the Japan Sea Proper Water, has very narrow ranges of temperature and salinity (WORTHINGTON, 1981),

---

Division of Earth Environment Dynamics,  
Research Institute for Applied Mechanics, Kyushu  
University  
6-1 Kasuga-Koen, Kasuga City, Fukuoka 816-8580,  
Japan  
e-mail: senjyu@riam.kyushu-u.ac.jp

which results in a buoyancy frequency on the same order of  $f$  (typically  $1.0\text{--}5.0 \times 10^{-4} \text{ s}^{-1}$  below 1000 m). These facts indicate that NIW in the abyssal Japan Sea have a narrow frequency range. In addition, tidal flows in the Japan Sea are generally weak (SENJYU *et al.*, 2005). This fact indicates little contamination from tidal motions. The weakness of tidal flows also indicates that the most of sub-diurnal variations in the Japan Sea are the near-inertial motions, which suggests that the intensity of the basin-scale thermohaline circulation in the sea is mainly controlled by the near-inertial flows associated with NIW, analogous to the global-scale thermohaline circulation.

One reason that the behavior of NIW in deep water has not been clarified is that deep flow observations with high spatial and temporal resolution are not common. For example, in the Japan Sea, it has been common in long-term current monitoring for serial single-layer current meters to be spaced at tens to hundreds of meters in the vertical, with 30–60 minute sampling intervals (SENJYU *et al.*, 2005). Therefore, we made special observations to capture NIW propagation in the abyssal Japan Sea, using a moored Acoustic Doppler Current Profiler (ADCP) set to a very short measurement interval. Although the period of observation was only about 2 days, we successfully observed vertical NIW propagation in the deep sea. This paper describes the results of the observation and discusses the NIW structure, propagation, and generation in the abyssal Japan Sea.

## 2. Observation

The ADCP (300 kHz Workhouse, Teledyne RDI) was deployed at Sta. SH in the Yamato Basin of the Japan Sea ( $38^{\circ} 17.05' \text{ N}$ ,  $135^{\circ} 50.06' \text{ E}$ ) at 07:12 on 13 May and recovered at 05:39 on 15 May 2013 by TR/V Nagasaki Maru of Nagasaki University (Fig. 1). The ADCP was moored

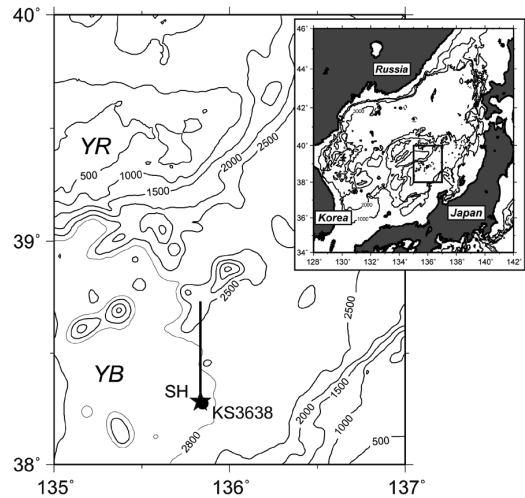


**Fig. 1** Observation site. Contour lines indicate water depth in meters. Star and circle indicate Sta. SH of ADCP mooring and Sta. KS3638 of JMA, respectively. YB and YR denote the Yamato Basin and Yamato Rise, respectively. The ray-tracing was done in the section along the solid line. The area is enlarged map of the square in the inset showing the Japan Sea.

upward looking at 2650 m. To detect NIW propagation, we set bin size and measurement intervals at 4 m (with the first bin at 6.2 m) and 10 seconds, respectively. The nominal accuracy of the ADCP is  $\pm 0.5\%$  of water velocity relative to the instrument  $\pm 0.5 \text{ cms}^{-1}$ . The accuracy and precision of flow direction are  $\pm 2.0^{\circ}$  and  $\pm 0.5^{\circ}$ , respectively.

The posture of ADCP during the observation was very stable. Pitch and roll angles monitored by a tilt sensor in the instrument were within  $\pm 1^{\circ}$  throughout the mooring period. Nevertheless, no flow data were obtained by the equipment for layers farther than 50 m because of weak acoustic echo intensity, though the nominal observation distance was set to 100 m. In addition, data at the first layer (2644 m) were noisy. Therefore, we analyzed the velocity profile in the 40 m range from 2600 to 2640 m (layers 2–12 of the

equipment, for a total of 11).

Six successive velocity profiles at 10-second intervals were averaged to yield 1-minute interval data. Furthermore, 5-minute running mean was applied to the 1-minute data to reduce short-term fluctuations. The size of the averaging time window (5-minute) was determined try and error to reserve the signal of vertical propagation of NIW. Owing to the averaging, standard deviation in a current measurement was reduced to  $0.16 \text{ cm s}^{-1}$ . The available data length is 45 hours 54 minutes from 07:43 on 13 May to 05:37 on 15 May 2013.

In addition to the flow observation, temperature at 2650 m was measured with a sensor embedded in the ADCP transducer head at the same sampling intervals as flows. Though the nominal precision of the sensor is  $\pm 0.4^\circ\text{C}$  and the accuracy and time constant of the sensor are unknown, the temperature measurements are useful for the present study because the relative values of temperature are available by the resolution of the sensor,  $0.01^\circ\text{C}$ . The same procedure of flows was applied to the temperature data.

### 3. Results

Time series of east-west ( $u$ ) and north-south ( $v$ ) components of velocities at 2604, 2620, and 2636 m are shown in Fig. 2, along with temperature measurements ( $T$ ) at 2650 m. Flows at each layer exhibited similar temporal variations to each other, showing a prevailing barotropic flow. Speed and direction of the vertically-averaged mean flow for the observation period were  $2.73 \text{ cm s}^{-1}$  and  $315.8^\circ$ , respectively. This northwestward flow may be part of the cyclonic circulation in the Yamato Basin (SENJYU *et al.*, 2005), though the observed flows showed a linear temporal trend.

A sinusoidal flow variation with a period of

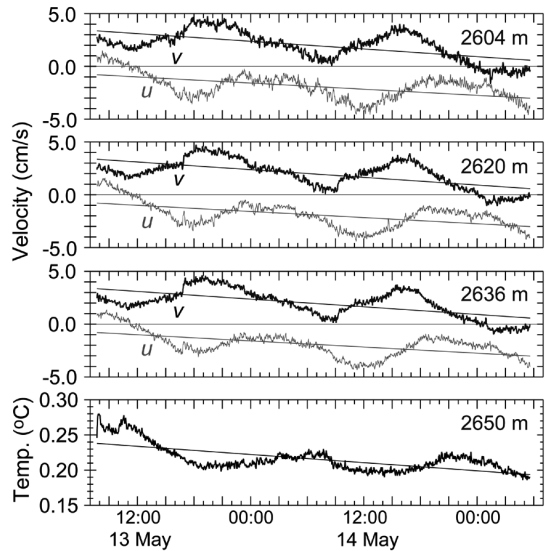


Fig. 2 Time series of velocity at 2604, 2620, and 2636 m and temperature at 2650 m. Gray thin and black bold lines in velocity show east-west ( $u$ ) and north-south ( $v$ ) components, respectively. Thin straight lines in each panel denote the linear trend throughout the observation period.

about 20 hours, superimposed on the linear trend, was clear in each layer. The phase of sinusoidal variation in  $v$  led by about  $90^\circ$  than that in  $u$ , showing a clockwise change of flow direction. Similar periodical variation to that of flows was found for temperature. In addition, vertically-coherent fluctuations with relatively large amplitude were occurred intermittently, for example a velocity shift in 16:30–17:00 on 13 May and a jump in  $v$  in 09:00–10:00 on 14 May. However, most of short period fluctuations in flow and temperature measurements are probably due to noise, which amplitudes are near the measurement threshold and tend to be large as increase of distance from the equipment.

For a rough estimate of the dominant period of variation, we separated the periodical components in  $u$ ,  $v$ , and  $T$  (hereafter  $u'$ ,  $v'$ , and  $T'$ ) from background variations by subtracting the tempo-

**Table 1** Mean relative angles of the velocity vector at each layer to the velocity at 2640 m

Depth (m)	2636	2632	2628	2624	2620	2616	2612	2608	2604	2600
Relative Angle (°)	0.86	1.83	0.88	2.06	2.47	1.54	2.29	3.06	3.93	3.17

ral linear trends from the measurements, then calculated auto-correlation functions for  $u'$ ,  $v'$ , and  $T'$ . The linear temporal trend for flows was calculated from the vertically-averaged flow by least square method. The estimated periods (frequencies) of  $u'$  and  $v'$  as the mean for the all observation depths were 1118.3 minutes ( $\omega_u = 9.364 \times 10^{-5} \text{ s}^{-1}$ ) and 1192.6 minutes ( $\omega_v = 8.781 \times 10^{-5} \text{ s}^{-1}$ ), respectively, and the estimated period (frequency) of  $T'$  at 2650 m was 1136 minutes ( $\omega_T = 9.218 \times 10^{-5} \text{ s}^{-1}$ ). Since the local inertial period (frequency) at the observation site is 1158.9 minutes ( $f = 9.036 \times 10^{-5} \text{ s}^{-1}$ ), the observed periodical variations of flows and temperature are mostly attributable to NIW. It may seem strange that the frequency of  $v'$  is lower than the local inertial frequency. This is likely due to an insufficiently long observation period for precise estimation of near-inertial motions, though a region of negative relative vorticity can trap sub-inertial frequency motions (KUNZE, 1985).

Because of the noisy short period fluctuations, it is hard to confirm the polarization relation in a snapshot profile of  $u'$  and  $v'$ . Therefore, we calculated the angles between the velocity vector at each layer and that at 2640 m (relative angles referred to the deepest layer velocity vector), and averaged them for the observation period (Table 1 and Fig. 3). The mean relative angles exhibited positive values throughout the observation depths, indicating a clockwise rotation of velocity vectors in the shallower layers. Furthermore, the mean relative angles tend to decrease from 3–4° at 2600–2608 m to less than 1° at 2628 and 2636 m. This polarization suggests a downward phase propagation of NIW (GILL,

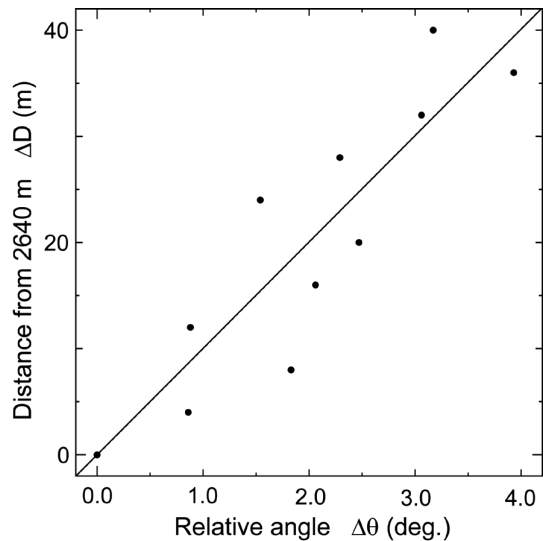


**Fig. 3** Relationship between the mean relative angles of velocity vector to that at 2640 m ( $\Delta\theta$ ) and the vertical distance from 2640 m ( $\Delta D$ ). The regression line is shown by the straight line.

1982). As a typical example of vertical NIW propagation, time-depth diagrams of  $u'$  and  $v'$  are shown in Fig. 4 for 11:00–17:00 on 14 May. Vertical phase propagation from upper to lower layers is discernible in both components. Similar vertical phase propagations in  $u'$  and  $v'$  to that in Fig. 4 were detected several times during the observation period.

## 4. Discussions

### 4.1 Structure of the NIW

At first, vertical phase speed and wave number of the NIW were tried to estimate from vertical cross-correlation functions for  $u'$  and  $v'$ . However, broad peaks in the cross-correlation functions prevented us from a reliable estimation.

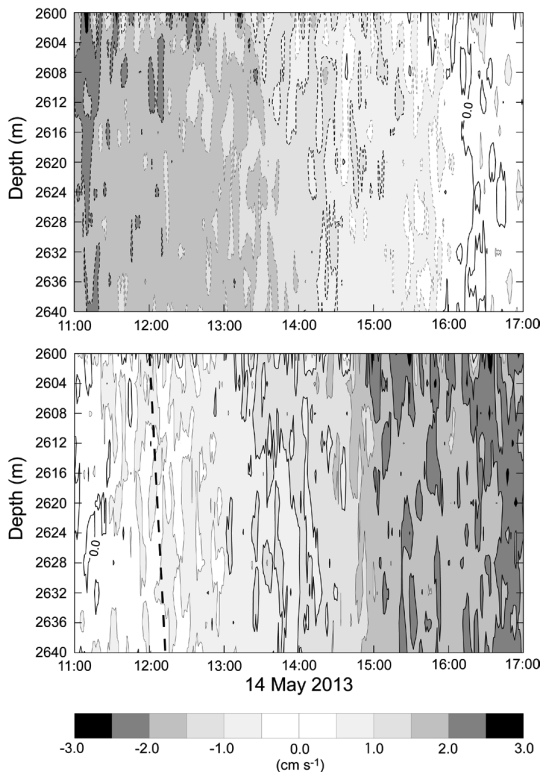


Fig. 4 Time-depth diagram for  $u'$  (upper) and  $v'$  (lower) during 11:00 to 17:00 on 14 May 2013. Negative values were denoted by dashed contours. Broken line in lower panel shows the estimated propagation speed  $5.34 \times 10^{-2} \text{ ms}^{-1}$ .

Therefore, we estimated the vertical wave length of the NIW from the polarization relation; Fig. 3 shows a clear linear relationship between the relative angle ( $\Delta\theta$ ) and distance from the reference depth 2640 m ( $\Delta D$ ), with the correlation coefficient of +0.89. The polarization relation determined by least square method is

$$\Delta D = 10.025 \times \Delta\theta \quad (1),$$

which shows the vertical wave length  $\lambda_z$  of 3609 m (vertical wave number  $= 1.741 \times 10^{-3} \text{ m}^{-1}$ ) as  $\Delta D$  at  $\Delta\theta = 360^\circ$ . If we take  $\omega = 9.291 \times 10^{-5} \text{ s}^{-1}$  as the mean of  $\omega_u$  and  $\omega_T$ , reasonable frequencies

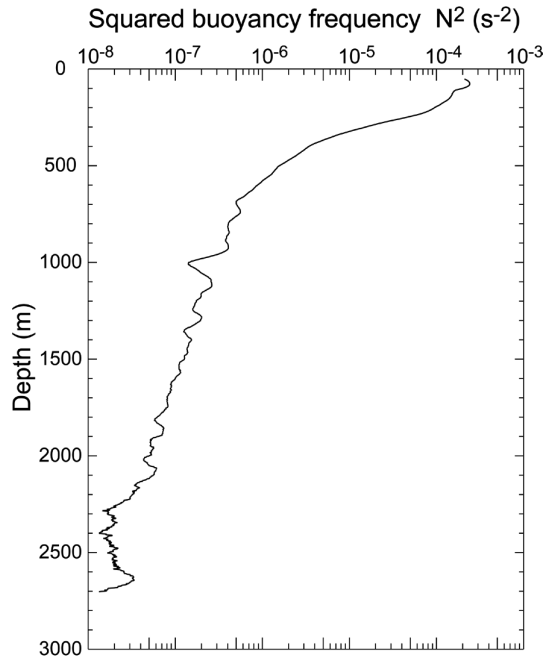


Fig. 5 Vertical profile of squared buoyancy frequency ( $N^2$ ) at Sta. KS3638 of JMA.

higher than the local inertial frequency at the observation site, then vertical phase speed  $C_z (= \omega/m)$  is estimated to be  $5.34 \times 10^{-2} \text{ ms}^{-1}$  (broken line in the lower panel of Fig. 4). Such fast phase propagations cannot be captured by typical deep-sea mooring observations with few current meters of tens to hundreds of meters vertical spacing and 30–60 minutes sampling intervals.

Unfortunately, there were no stratification data near the observation site during the mooring period. Therefore, we inferred squared buoyancy frequency  $N^2$  in the abyssal Yamato Basin from temperature and salinity data at Sta. KS3638 ( $38^\circ 16.52' \text{ N}$ ,  $135^\circ 50.69' \text{ E}$ ), obtained by the Japan Meteorological Agency (JMA) on 4 November 2012 (Fig. 1).  $N^2$  from 2600 to 2640 m is  $2.554\text{--}3.385 \times 10^{-8} \text{ s}^{-2}$  (Fig. 5), with mean  $3.022 \times 10^{-8} \text{ s}^{-2}$  corresponding to the buoyancy frequency (period) of  $1.739 \times 10^{-4} \text{ s}^{-1}$  (602.4 minutes).

Using the values of  $f$ ,  $\omega$ , and  $N^2$  above, the phase

propagation angle of the NIW from the horizontal ( $\varphi$ ) was estimated at  $81.6^\circ$  from

$$\tan^2\varphi = \frac{N^2 - \omega^2}{\omega^2 - f^2} = 46.13 \quad (2).$$

Since the above relationship also represents the aspect ratio of NIW ( $m^2/\kappa_H^2$ , where  $\kappa_H$  is horizontal wave number),  $\kappa_H$  of the observed NIW was estimated to be  $2.563 \times 10^{-4} \text{ m}^{-1}$  (horizontal wave length  $\lambda_H=24512 \text{ m}$ ).

#### 4.2 Propagation of the NIW

Since phase propagation of the observed NIW was directed from upper to lower layers, the direction of the group velocity must be upward according to the linear wave theory (GILL, 1982). This suggests that the observed NIW were generated at the seabed or were bottom-reflected waves. To examine the bottom generation/reflection possibility, we back-traced the NIW energy ray from the observation site. The WKB approximation is not applicable because of the large vertical wave length of the NIW comparable to the length scale of density stratification  $N$ . However, variation of  $N$  is on the order of  $10^{-4} \text{ s}^{-1}$  below 1000 m (from  $1.153 \times 10^{-4} \text{ s}^{-1}$  near the bottom to  $5.140 \times 10^{-4} \text{ s}^{-1}$  at 1116 m, Fig. 5). Therefore, we considered that  $N$  is almost constant and assumed that the ray-tracing method is locally applicable below 1000 m.

Since NIW can only freely propagate equatorward from its generation area (GARRETT, 2001) and the critical latitude at which the local inertial frequency  $f$  is the same as the observed NIW frequency  $\omega$  is  $39^\circ 35.3' \text{ N}$ , the generation or reflection region of the observed NIW is likely to be north of the observation site. Therefore, tentatively, the backward ray-tracing was done northward in the section along  $135^\circ 50.0' \text{ E}$  with origin  $38^\circ 17.0' \text{ N}$  (observation site) on the  $\beta$ -plane, assuming the profile of  $N^2$  at Sta. KS3638 of JMA

for the entire region (Fig. 1). Southward propagation of the observed NIW is qualitatively supported by the relationship between  $\nu'$ , and  $T'$  in Fig. 2; when  $\nu'$  was negative (southward)  $T'$  tended to decrease because of upward advection of cold water in the lower layer, and vice versa (see Fig. 8.4 in GILL, 1982).

The ray-tracing shows that the NIW passing through a point 2620 m of the observation site with upward group velocity are bottom-reflected waves (Fig. 6), which were downward-propagating NIW incident on the bottom about 1.1 km north of the observation site. Further back-tracing suggests that the observed NIW were generated in the upper layer, rather than the seabed around the observation site.

#### 4.3 Generation of the NIW

It has been reported that near-inertial motions observed in the upper layer of the Japan Sea were associated with atmospheric disturbances (KIM *et al.*, 2005; OKEI *et al.*, 2009; IGETA *et al.*, 2009, 2011). Part of the near-inertial motions generated in the upper layer can propagate down into the deep layer (ALFORD *et al.*, 2012), though most of wind energy injected into the ocean is confined in the surface mixed layer (FURUICHI *et al.*, 2008). Therefore, we examined wind conditions before and during the observation period using the Grid Point Value/Meso Spectral Model (GPV/MSM) data provided from JMA. The GPV/MSM is hourly operational weather forecasting data with spatial resolutions of  $0.05^\circ$  and  $0.0625^\circ$  in latitude and longitude, respectively.

The time series of wind speed averaged over the area in Fig. 1 ( $38^\circ\text{--}40^\circ \text{ N}$ ,  $135^\circ\text{--}137^\circ \text{ E}$ ) is shown in Fig. 7a for the period of 8–15 May 2013. Although the wind speed was less than  $10 \text{ ms}^{-1}$  throughout the analysis period, a marked event occurred in 10–11 May. Fig. 7b shows the time series of wind vectors for the 20-hour high-pass

filtered component including the local inertial period variations. A clockwise change in wind direction is clear during the period from 13:00 on May 10 to 12:00 on May 11. This clockwise change in wind direction was dominant variation because the high-pass filtered component accounts for

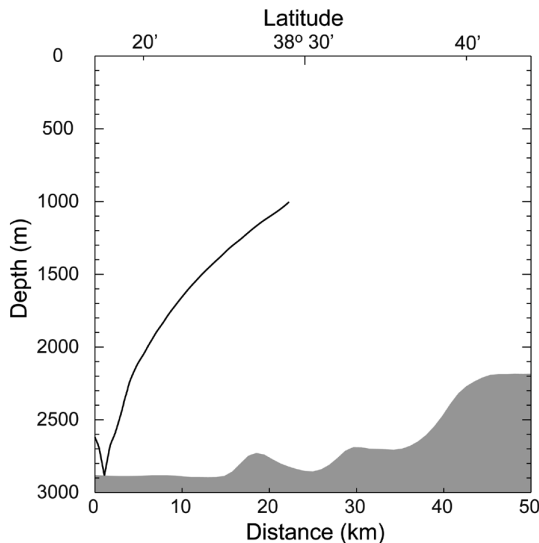


Fig. 6 Ray path of the southward propagating NIW passing through a point 2620 m of the observation site in the section along the solid line in Fig. 1.

more than 40% of the total wind speed in this period (Fig. 7a). Since surface near-inertial currents are most efficiently enhanced when wind vector rotates inertially (LARGE and CRAWFORD, 1995), this atmospheric event may be a cause of the observed NIW.

Another possible process of the NIW generation is geostrophic adjustment accompanied with instabilities of the mean flow (TANG, 1979). North of the observation site, the subarctic front in the Japan Sea lies about  $40^{\circ}$  N with significant variability due to mesoscale eddies generated by instability (ISODA, 1994). Besides, internal lee waves may be excited by interactions between deep flows and the Yamato Rise (NIKURASHIN and FERRARI, 2010), because the subarctic front intersects the Yamato Rise throughout the year (PARK *et al.*, 2007) and the mesoscale fluctuations in the subarctic front influence the deep flow field (SENJYU *et al.*, 2013). The high level of internal wave energy in the Yamato Basin (MORI *et al.*, 2005; SHCHERBINA *et al.*, 2003) is partly attributable to the instability of flows along the subarctic front and the Yamato Rise. However, the observed NIW may be not the case because of its large

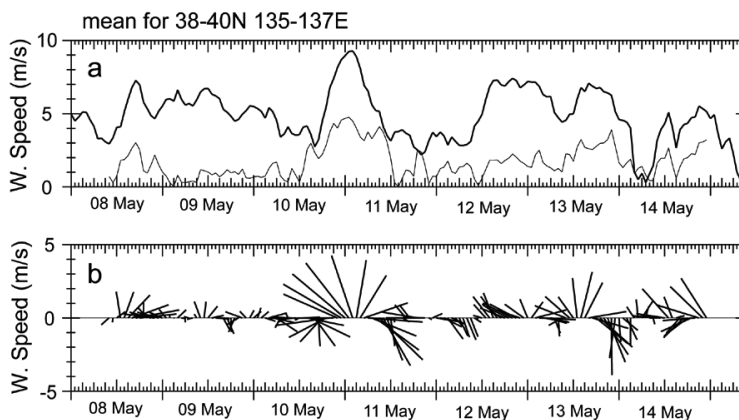


Fig. 7 Time series of the GPV/MSM wind averaged over the area  $38^{\circ}$ – $40^{\circ}$  N,  $135^{\circ}$ – $137^{\circ}$  E (Fig. 1) for the period of 8–15 May 2013. (a) Wind speed (bold line) and that for the 20-hour high-pass filtered component (thin line). (b) Wind vectors for the 20-hour high-pass filtered component.

vertical wave length; it has been reported that the vertical scale of internal lee waves excited by interactions between deep flows and topography are  $\sim 600$  m (NIKURASHIN and FERRARI, 2010).

## 5. Remarks

Vertical propagation of NIW was observed in the abyssal Japan Sea, where a barotropic flow generally prevails. It is feasible to use the detailed flow structure revealed by moored-ADCP observation of high spatial and temporal resolution to elucidate mixing processes in the deep ocean interior. Although vertical shears during the observation period were relatively stable, typically on the order of  $10^{-3} \text{ s}^{-1}$ , seasonal and intermittent intensifications of near-inertial flows have been reported in the abyssal Japan Sea (MORI *et al.*, 2005). Strong vertical shear promoting oceanic mixing is possible during such periods.

The horizontal wave number and propagation angle of NIW were estimated from equation (2) which relates wave parameters  $m$ ,  $\kappa_H$ , and  $\varphi$  with  $\omega$ . In particular, the propagation angle  $\varphi$  depends sensitively on  $\omega$ , because the denominator of equation (2) becomes very small for NIW. However, since our observation period was only about 46 hours, 2.4 times of the local inertial period, we could not estimate  $\omega$  precisely, posing major limitation of this study. Precise estimation of  $\omega$  based on longer-period observation remains as a problem to be solved in future.

## Acknowledgments

We would like to thank the captain and crew of the TR/V Nagasaki Maru and Mr. T. Mada for help in the observation field. Profs. T. MATSUNO, H. -R. SHIN, and Dr. T. Endo are acknowledged for useful discussions. The comments from two anonymous reviewers were helpful for the revision of the manuscript. The GPV/MSM data

used in this study were NetCDF files provided from Research Institute for Sustainable Humansphere, Kyoto University. Part of this study was supported by JSPS KAKENHI Grant Number 26610151.

## References

- ALFORD, M.H., M.F. CRONIN and J.M. KLYMAK (2012): Annual cycle and depth penetration of wind-generated near-inertial waves at ocean station Papa in the Northeast Pacific. *J. Phys. Oceanogr.*, **42**, 889–909.
- BYUN, S.S., J.J. PARK, K.I. CHANG and R.W. SCHMITT (2010): Observation of near-inertial wave reflections within the thermocline layer of an anticyclonic mesoscale eddy. *Geophys. Res. Lett.*, **37**, L01606, doi:10.1029/2009GL041601.
- FU, L.L. (1981): Observations and models of internal waves in the deep ocean. *Rev. Geophys. Space Phys.*, **19**, 141–170.
- FURUICHI, N., T. HIBIYA and Y. NIWA (2008): Model-predicted distribution of wind-induced internal wave energy in the world's ocean. *J. Geophys. Res.*, **113**, C09034, doi: 10.1029/2008JC004768.
- GAMO, T. and Y. HORIBE (1983): Abyssal circulation in the Japan Sea. *J. Oceanogr. Soc. Japan*, **39**, 220–230.
- GARRETT, C. (2001): What is the “near-inertial” band and why is it different from the rest of the internal wave spectrum? *J. Phys. Oceanogr.*, **31**, 962–971.
- GILL, A. E. (1982): *Atmosphere-Ocean Dynamics*. Academic Press, Orlando, 662 pp.
- HIBIYA, T., Y. NIWA, K. NAKAJIMA and N. SUGINOHARA (1996): Direct numerical simulation of the roll-off range of internal wave shear spectra in the ocean. *J. Geophys. Res.*, **101** (C6), 14123–14129, doi: 10.1029/96JC01001.
- IGETA, Y., Y. KUMAKI, Y. KITADE, T. SENJYU, H. YAMADA, T. WATANABE, O. KATOH and M. MATSUYAMA (2009): Scattering of near-inertial internal waves along the Japanese coast of the Japan Sea. *J. Geophys. Res.*, **114**, C10002, doi: 10.1029/2009JC005305.
- IGETA, Y., T. WATANABE, H. YAMADA, K. TAKAYAMA and O. KATOH (2011): Coastal currents caused by

- superposition of coastal-trapped waves and near-inertial oscillations observed near the Noto Peninsula, Japan. *Cont. Shelf Res.*, **31**, 1739–1749.
- ISODA, Y. (1994): Warm eddy movements in the eastern Japan Sea. *J. Oceanogr.*, **50**, 1–15.
- KANARI, S., M. KOGA, K. TAKEUCHI and M. TSUJI (1987): Near-inertial internal waves in the area off Yoichi coast of Hokkaido. *Geophys. Bull. Hokkaido Univ.*, **49**, 369–379.
- KIM, H.J., Y.G. PARK and K. KIM (2005): Generation mechanism of near-inertial internal waves observed off the east coast of Korea. *Cont. Shelf Res.*, **25**, 1712–1719.
- KIM, H.R., S. AHN and K. KIM (2001): Observations of highly nonlinear internal solitons generated by near-inertial internal waves off the east coast of Korea. *Geophys. Res. Lett.*, **28**(16), 3191–3194.
- KUNZE, E. (1985): Near-inertial wave propagation in geostrophic shear. *J. Phys. Oceanogr.*, **15**, 544–565.
- LARGE, W.G. and G.B. CRAWFORD (1995): Observations and simulations of upper-ocean response to wind events during the Ocean Storms Experiment. *J. Phys. Oceanogr.*, **25**, 2831–2852.
- LIE, H.J. (1988): Near-inertial current oscillations off the mid-east coast of Korea. *Prog. Oceanogr.*, **21**, 241–253.
- MORI, K., T. MATSUNO and T. SENJYU (2005): Seasonal/spatial variations of the near-inertial oscillations in the deep water of the Japan Sea. *J. Oceanogr.*, **61**, 761–773.
- NIKURASHIN, M. and R. FERRARI (2010): Radiation and dissipation of internal waves generated by geostrophic motions impinging on small-scale topography: theory. *J. Phys. Oceanogr.*, **40**, 1055–1074.
- OKEI, N., J. OKUNO and T. SENJYU (2009): Kyucho around the Noto Peninsula induced by the passage of meteorological disturbances, the observations in summer 2003. *Oceanogr. in Japan*, **18**, 57–69.
- PARK, J. H. and D. R. WATTS (2005): Near-inertial oscillations interacting with mesoscale circulation in the southwestern Japan/East Sea. *Geophys. Res. Lett.*, **32**, L10611, doi: 10.1029/2005GL022936.
- PARK, K.A., D.S. ULLMAN, K. KIM, J.Y. CHUNG and K.R. KIM (2007): Spatial and temporal variability of satellite-observed subpolar front in the East/Japan Sea. *Deep-Sea Res. I*, **54**, 453–470.
- SENJYU, T., T. ARAMAKI, S. OTOSAKA, O. TOGAWA M. DANCHENKOV, E. KARASEV and Y. VOLKOV (2002): Renewal of the bottom water after the winter 2000–2001 may spin-up the thermohaline circulation in the Japan Sea. *Geophys. Res. Lett.*, **29**(7), doi: 10.1029/2001GL014093.
- SENJYU, T., H.R. SHIN, J.H. YOON, Z. NAGANO, H.S. AN, S.K. BYUN and C.K. LEE (2005): Deep flow field in the Japan/East Sea as deduced from direct current measurements. *Deep-Sea Res. II*, **52**, 1726–1741.
- SENJYU, T., T. ARAMAKI, S.S. TANAKA, J. ZHANG, Y. ISODA, Y. KUMAMOTO, S. HIBINO and T. NAKANO (2013): Abyssal water mass exchange between the Japan and Yamato Basins in the Japan Sea. *J. Geophys. Res. Ocean*, **118**, 4878–4888, doi: 10.1002/jgrc.20373.
- SHCHERBINA, A.Y., L.D. TALLEY, E. FIRING and P. HACKER (2003): Near-surface frontal zone trapping and deep upward propagation of internal wave energy in the Japan/East Sea. *J. Phys. Oceanogr.*, **33**, 900–912.
- TAKEMATSU, M., Z. NAGANO, A.G. OSTROVSKII, K. KIM and Y. VOLKOV (1999): Direct measurements of deep currents in the northern Japan Sea. *J. Oceanogr.*, **55**, 207–216.
- TANG, C.L. (1979): Inertial waves in the Gulf of St Lawrence: a study of geostrophic adjustment. *Atmos.-Ocean*, **17**, 135–156.
- TOOLE, J.M. and T.J. McDOUGALL (2001): Mixing and stirring in the ocean interior. *In Ocean Circulation and Climate*, Siedler, G., J. Church and J. Gould (eds.), Academic Press, San Diego, p. 337–355.
- WEBSTER, F. (1968): Observations of inertial period motions in the deep sea. *Rev. Geophys. Space Phys.*, **6**, 473–490.
- WORTHINGTON, L.V. (1981): The water mass of the world ocean: some results of a fine-scale census. *In Evolution of Physical Oceanography*, Warren, B.A. and C. Wunsch (eds.), M.I.T. Press, Cambridge, p. 42–69.

Received: April 7, 2015

Accepted: October 2, 2015

